

The “False Colour” Problem

Jean Serra

Université Paris-Est, Laboratoire d'Informatique Gaspard Monge, Equipe A3SI,
ESIEE Paris, France
j.serra@esiee.fr

Abstract. The emergence of new data in multidimensional function lattices is studied. A typical example is the apparition of false colours when (R,G,B) images are processed. Two lattice models are specially analysed. Firstly, one considers a mixture of total and marginal orderings where the variations of some components are governed by other ones. This constraint yields the “pilot lattices”. The second model is a cylindrical polar representation in n dimensions. In this model, data that are distributed on the unit sphere of $n - 1$ dimensions need to be ordered. The proposed orders, and lattices are specific to each image. They are obtained from Voronoi tessellation of the unit sphere. The case of four dimensions is treated in detail and illustrated.

1 Introduction

When one takes the supremum of two numerical functions f and g , the resulting function $f \vee g$ may largely differ from the two operands, though at each point x the supremum $(f \vee g)(x)$ equals either $f(x)$ or $g(x)$. In multidimensional cases, the situation becomes worse. If our two functions now represent colour vectors, their supremum at point x may be neither $f(x)$ nor $g(x)$. A false colour is generated. This parasite phenomenon, due to the multidimensionality of our working space, appears therefore when dealing with satellite data, or with the composite data of the geographical information systems.

The present study aims to analyze, and, if possible, to control the phenomenon. In such matter one rarely finds a unique good solution, but usually several attempts, more or less convincing. In this respect, the case of colour imagery, and the associated lattices, turns out to be an excellent, and very visual, paradigm for multidimensional situations. It has motivated many approaches, from which one can extract the three following themes.

The first theme deals with the advantages and disadvantages of a total ordering for multivariate data. For some authors, this ordering seems to be an absolute requirement, which should be satisfied by lexicographic means [5] [14]. By so doing, one favours the priority variable to the detriment of the second, and so on. By reaction, other authors observe that total ordering in \mathbb{R}^1 has the two different finalities of *i*) locating the extrema, and *ii*) defining distances between grey levels. When passing from grey to colour, i.e. from \mathbb{R}^1 to \mathbb{R}^3 , it may be advantageous to dissociate the two roles. Numbers of markers can replace

extrema, and numbers of distances can describe vector proximity. This point of view, clearly explicit in [8], led A.Evans and D.Gimenez to remarkable connected filters for colour images, and F. Meyer to a watershed algorithm for colour images [11].

However, a total ordering is sometimes necessary, e.g. when we work in a space for which hue is not a coordinate. As we saw, in the usual product lattice $R \times G \times B$, the supremum of two triplets (r, g, b) may have a hue different from that of the two operands. One could argue that it suffices to take cylindrical coordinates, i.e. to replace R, G, B by L, S, H (for luminance, saturation, hue), equipped with a correct norm, such as L_1 or $\max - \min$ [1], to bring down the objection, since the hue is then directly under control. But this solution ignores that the higher is saturation, the more hue is significant. If the pixel with the highest hue has also a low saturation, the former is practically invisible, though it can be strongly amplified by a product of suprema, just as if it was a false colour. In conclusion, let us say that the matter is less keeping or not a total ordering than ensuring that some variables must not be treated separately. For example, we could demand that the hue of the supremum be that of the pixel with the highest saturation. Then the latter “pilots” the hue, hence the name of this ordering, and of the associated lattices. They are studied below in section 3.

Now, when passing from the Euclidean representation R, G, B to a polar system such as L, S, H , we introduce new drawback. On the unit circle, the hue ordering is not only arbitrary, but also the cause of a strong discontinuity between violet and red. How to master this parasite effect? One can imagine several strategies. For example, we may restrict ourselves to use increments only [9], or we may take several origins for the hue, according to its histogram, as proposed by E.Aptoula and S.Lefèvre in [3], [4]. We may make the hue depend on some neighborhood around each pixel, and not on the whole image, etc.. For multivariate data in n dimensions, the same problem reappears, now on the unit sphere in \mathbb{R}^n . Section 4 below proposes to segment this unit sphere by means of Voronoi polyhedra, which generalizes the method of Aptoula and Lefèvre .

Finally the third theme, typical of multivariate data, consists in using some variables for mixing the segmentations of other ones. For example, P. Soille considers a hierarchy of partitions and extracts at each level the classes that satisfy a constraining criterion [13]. The quaternions algebra offers another way, investigated by T.A. Ell and S.J. Sangwine [7] for Fourier transform of colour images, where the real axis is particularized. In [1] J.Angulo and J. Serra segment separately the three grey images H, L , and S , and then keep either hue or luminance segmentation, according as saturation is high or low. This mode of classification is extended to more dimensions in the example of remote sensing presented in section 6.

The three above themes lie on the implicit assumption of finiteness of the data sets, as they resort to Proposition 2 below. But the usual working spaces \mathbb{R}^2 and \mathbb{Z}^2 are not finite. How to reconcile the two points of view? This initial mathematical step will be the matter of the next section.

2 Lattices of Finite Parts

Proposition 2 imposes we restrict ourselves to *finite* families of points only. But if we take for framework a given finite part of \mathbb{R}^n or \mathbb{Z}^n , we have to renounce to translation invariance, hence to Minkowski operations. Observe however that the problem is not working with the subsets of a finite set, but working with finite sets that remain finite under the operations that transform them.

Set case. A good way for expressing this idea consists in starting from an arbitrary set E , possibly finite, countable, or even continuous, and focusing on its finite parts exclusively. As they are closed under intersection, with \emptyset as smallest element, we just need to provide them with a universal upper-bound, namely E itself, for obtaining a complete lattice. Hence we can state [12].

Proposition 1. Set lattice of finite parts (LFP): *Let E be a set, and let \mathcal{X}' be the class of its finite parts. The set $\mathcal{X} = \mathcal{X}' \cup E$ forms a complete lattice for inclusion ordering, where, for every family $\{X_i, X \in \mathcal{X}, i \in I\}$, possibly infinite, the infimum $\wedge X_i$ and the supremum $\vee X_i$ are given by*

$$\begin{aligned} \wedge X_i &= \cap X_i, \\ \vee X_i &= \cup X_i \text{ when } \cup X_i \text{ is upper-bounded by an element of } \mathcal{X}', \\ \vee X_i &= E \text{ when not.} \end{aligned}$$

Class \mathcal{X} is closed under infimum, since even when I is the empty family, we have that $\wedge \{X_i, i \in \emptyset\} = E \in \mathcal{X}$. Proposition 1 applies for sets of points with integer coordinates in \mathbb{Z}^n or in \mathbb{R}^n , as well as for infinite graphs.

Function case. Before extending Proposition 1 to numerical functions, we recall a classical result on ordered sets.

Proposition 2. *Let T be an ordered set. Every finite family $\{t_i, i \in I\} \in T$ admits a supremum $\vee t_i$ and an infimum $\wedge t_i$ which are themselves elements of the family iff the ordering of T is total.*

The proposition cannot be generalized to countable families, even neither to finite families when the ordering is partial only (e.g. $R \times G \times B$ colour space). In the following, the set T of Proposition 2 is a numerical lattice, and corresponds to the arrival space of the functions under study. It may be $\overline{\mathbb{R}}$, or a closed part of $\overline{\mathbb{R}}$, or $\overline{\mathbb{Z}}$, or any subset of $\overline{\mathbb{Z}}$. The two universal bounds of T are denoted by M_0 and M_1 . As we did for $\mathcal{P}(E)$ with Proposition 1, we can associate with T a finite lattice \mathcal{T} . It suffices to put, for any family $\{t_j, j \in J\}$ in T , that

$$\begin{aligned} \wedge \{t_j, j \in J\} &= \wedge t_j \text{ when } \text{Card}(J) < \infty, \text{ and } \wedge \{t_j, j \in J\} = M_0 \text{ when not,} \\ \vee \{t_j, j \in J\} &= \vee t_j \text{ when } \text{Card}(J) < \infty, \text{ and } \vee \{t_j, j \in J\} = M_1 \text{ when not.} \end{aligned}$$

Lattice \mathcal{T} is made of all finite families of numbers, plus M_0 and M_1 . Consider now the class \mathcal{F} of all functions $f : E \rightarrow \mathcal{T}$ with a finite support. Finiteness must hold not only on the support of f and on $f(x)$, but also on the number of values taken at point x by any family $f_j \in \mathcal{F}$. This constraints lead to the following function lattice [12].

Proposition 3. Function lattice of finite parts : the class \mathcal{F} of functions $f : E \rightarrow \mathcal{T}$ with finite extrema and finite support forms a complete lattice for the pointwise numerical ordering. At point $x \in E$ the infimum \wedge and the supremum \vee of a finite or not family $\{f_j, j \in J\}$ in \mathcal{F} , are given by the expressions

$$\begin{aligned} (\wedge \{f_j, j \in J\})(x) &= \wedge f_j(x) \quad \text{when } x \in \cap X_j, \text{ and card } J \text{ are finite,} \\ (\wedge \{f_j, j \in J\})(x) &= M_0 \quad \text{when not;} \\ (\vee \{f_j, j \in J\})(x) &= \vee f_j(x) \quad \text{when } x \in \cup X_j \subseteq \mathcal{X}', \text{ and card } J \text{ are finite,} \\ (\vee \{f_j, j \in J\})(x) &= M_1 \quad \text{when not.} \end{aligned}$$

Lattice \mathcal{F} , and its multidimensional versions, are shared by all models we develop from now on, even when it is not explicitly recalled.

3 Pilot Lattices

This section is devoted to the first theme met in introduction, and to its consequence on “false colours”. We now work in the n dimensional space $T^{(n)}$, $n < \infty$. Its elements are the ordered sequences of n real numbers called components. The space $T^{(n)}$ can welcome many ordering relations leading to complete lattices, two extreme representatives of which being the marginal ordering and the lexicographic one. The first one is the product ordering of each component, and the second one describes a route over the whole space, where the first component is priority, then the second, the third, etc..If $t^1, t^2 \in T^{(n)}$, with $t^1 = (t_1^1, t_2^1, \dots, t_n^1)$, and $t^2 = (t_1^2, t_2^2, \dots, t_n^2)$, we get

– for the marginal ordering:

$$t^1 \leq t^2 \text{ iff } t_i^1 \leq t_i^2, \quad 1 \leq i \leq n$$

hence

$$\vee \{t^j, j \in J\} = (\vee t_1^j, \vee t_2^j, \dots, \vee t_n^j), \quad j \in J.$$

When family J is finite, each component of the supremum is a t_i^j , (Proposition 2), but taken from a point j that may be different for each component.

– for the lexicographic ordering

$$t^1 \leq t^2 \text{ iff } \exists i \text{ such that } t_i^1 < t_i^2 \text{ and } j < i \text{ imply } t_j^1 = t_j^2 \quad (1)$$

In other words, the order is obtained by comparing the leftmost coordinate on which the vectors differ. The ordering being now total, the supremum $\vee \{t^j, j \in J\}$ of any finite family J is one of its elements $t^j = (t_1^j, t_2^j, \dots, t_n^j)$ with all its components (Proposition 2).

The pilot structures take place between these two extremes. $T^{(n)}$ be a n -numerical space, and let a partition of $T^{(n)}$ into k complementary sub-spaces.

Definition 1. . Let $\{T_s^{(n)}, 1 \leq s \leq k\}$ be a family of function lattices of finite parts that are totally ordered. Their direct product, endowed with the marginal ordering is called Pilot lattice.

The pure marginal case is obtained for $k = n$, and the total ordering for $k = 1$. Except for marginal ordering, the supremum and infimum of any family always involve several components of some same elements of the family. Therefore they do not ensure us to completely preserve the initial data, but some of their components only. The next section gives examples of pilot lattices.

4 Polar Ordering in \mathbb{R}^n

We now develop the second theme pointed out in introduction. The idea is now to build a pilot lattice for cylindrical coordinates in \mathbb{R}^n , where the unit sphere be equipped with a significative total ordering [12].

Luminance and saturation. Colour polar representations are of cylindric type in \mathbb{R}^3 . The main diagonal stands for the cylinder axis, and its basis is given by the chromatic disc. The colour point (r, g, b) is projected in x^l on the axis, and in x^s on the base, and the so-called polar representations consist in various quantizations of these two projections. The generalization to \mathbb{R}^n is straightforward. Let $(x_1 \dots x_n)$ be the multispectral coordinates of point x , and x^l (resp. x^s) be its projection on the main diagonal D (resp. on the plane Π orthogonal to D passing by the origin O). Introduce the mean $m = \frac{1}{n} \sum x_i$. Point x^l has all its coordinates equal to m . As for point x^s , its coordinates satisfy the equation $\sum x_i^s = 0$, because vectors Ox^l and Ox^s are orthogonal, and also the $n - 1$ equations

$$x_1 - x_1^s = x_2 - x_2^s = \dots = x_n - x_n^s,$$

telling that x is projected parallel to the main diagonal. Hence,

$$x_i^s = \frac{1}{n} \left[(n-1)x_i - \sum_1^{n-1} x_i^s \right] = x_i - m \quad 1 \leq i \leq n. \quad (2)$$

According to the chosen norm, such as L_1 or L_2 , the “luminance” (resp. the “saturation”) is given by the average of the absolute values, or the quadratic average of the coordinates of x^l (resp. x^s). In the “chromatic” plane Π , vector x^s is expressed in spherical coordinates, i.e. by one module (the saturation) and by $n - 2$ directions (the hues), since $n - 2$ angles $\alpha_1 \dots \alpha_{n-2}$ are needed for locating a point on the unit sphere S_{n-1} in $n - 1$ dimensions.

Hues. We purpose to construct a pilot lattice from the product of three total orderings on luminance, saturation and hues. For the first two ones, which are energies, a usual numerical lattice is convenient. It remains to model the hues. Aptoula-Lefèvre ordering [3], [4] can be generalized as follows.

Let $\{c^j, 1 \leq j \leq k\}$ be a finite family of poles on S_{n-1} , of coordinates c_i^j , $1 \leq i \leq n - 1$. Just as in two dimensions, we use the notation $c \div c^j$ to indicate

the value of the acute angle cOc^j (i.e. $\leq \pi$) between point c and pole c^j . Take, on the unit sphere S_{n-1} , the Voronoï polygons w.r. to poles c^j , and assign for each point of the sphere the distance to its closest pole. In case of several equidistant poles, a priority rule allows to decide between them: conventionally c_1 prevails over c_2 , which prevails over c_3 etc.. Finally, in case of two points equidistant from a same pole α , we iterate the process in the unit sphere S_{n-2} orthogonal axis $O\alpha$, and possibly in S_{n-3} etc., until we find an angle inequality. Then we say that c is closer to its pole than c' is closer to its own one, and we write $c \sqsupseteq c'$ when

$$\text{either } \min_j \{c \div c^j\} < \min_p \{c' \div c^p\} \quad 1 \leq j, p \leq k, \quad (3)$$

$$\text{or } \min_j \{c \div c^j\} = c \div c^{j_0} = \min_p \{c' \div c^p\} = c' \div c^{p_0} \quad \text{and } j_0 > p_0, \quad (4)$$

$$\text{or } \min_j \{c \div c^j\} = c \div c^{j_0} = \min_p \{c' \div c^p\} = c' \div c^{j_0} \quad \text{and iteration in } S_{n-2}. \quad (5)$$

The last condition may seem complicated, but it considerably simplifies in the useful case of \mathbb{R}^4 . The three conditions classify points on the unit sphere according a total ordering based on angular interval, which can be replaced by any angular distance. The physical meaning here is the same as the resemblance to reference hues in the colour case.

Finally, we have in hand three finite total orderings: two numerical ones for luminance and saturation, plus ordering \sqsupseteq for the hues. Propositions 1 and 3 apply, and provide the multivariate data with a pilot lattice.

Choice of the initial data. Formally speaking, this pilot lattice allows us to segment in a space with more than 100 dimensions as those that occur in satellite imagery [6]. However, the strong redundancy of the bands makes that processing cumbersome. Indeed, one rarely finds, in literature on remote sensing, image processing involving more than 4 principal components. On the other hand, the situation is now different from the colour case, as the first component is by construction the most important one. Therefore, it seems more appropriate to consider it as the main diagonal (the “grey tones”).

Case of four components. We now develop in detail the four dimensional case, when the first components of a multi-spectral image are w, x, y, z . The first principal component w is chosen as the luminance, and describes the main diagonal in \mathbb{R}^4 . The coordinates of the luminance and saturation vectors are given by

$$x^l = (w, 0, 0, 0) \quad \text{and} \quad x^s = (0, x, y, z)$$

with $x, y, z \geq 0$. Hyperplane Π is nothing but the space \mathbb{R}^3 , and the polar cylindrical coordinates in Π nothing but the usual spherical ones of \mathbb{R}^3 . This context suggests to adopt the L_2 norm, since then the expressions of the saturation and of the two hues are those of the module ρ , the colatitude θ and the longitude ψ of the usual spherical coordinates in \mathbb{R}^3 , i.e.

$$\rho = \sqrt{x^2 + y^2 + z^2} \quad (6)$$

$$\cos \theta = \frac{z}{\rho}, \quad \cos \psi = \frac{x}{\rho \sin \theta}, \quad \sin \psi = \frac{y}{\rho \sin \theta}. \quad (7)$$

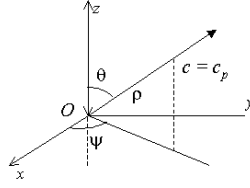


Fig. 1. Polar coordinates (ρ, θ, ψ) of point c , itself projection c_p of a point in R^4

Both colatitude θ and longitude ψ vary from 0 to $\frac{\pi}{2}$ since $x, y, z \geq 0$. These angles are depicted in Fig.1. Let $\{c^j, 1 \leq j \leq k\}$ be k poles on the unit sphere, ordered by decreasing priorities, and with coordinates $c^j = (x^j, y^j, z^j)$.

The angle cOc^j between point c and pole c^j is bounded by 0 and $\pi/2$. One obtains it from the scalar product of the two vectors c and c^j

$$\cos(cOc^j) = \langle c, c^j \rangle = \frac{xx^j + yy^j + zz^j}{\rho\rho^j}. \quad (8)$$

This relation allows us to re-formulate the first two relations (3) and (4) of the hue ordering in a simpler manner. We have $c \supseteq c'$ when

$$\text{either } \min_j \{\langle c, c^j \rangle\} > \min_p \{\langle c', c^p \rangle\} \quad 1 \leq j, p \leq k, \quad (9)$$

$$\text{or } \min_j \{\langle c, c^j \rangle\} = \langle c, c^{j_0} \rangle = \min_p \{\langle c', c^p \rangle\} = \langle c', c^{p_0} \rangle \quad \text{and } j_0 < p_0. \quad (10)$$

The third relation (5) corresponds to the case when c and c' are equidistant to their closest pole c^{j_0} . Then they can be ordered by increasing longitudes ψ . Finally, if $\psi(c) = \psi(c')$, what happens when c, c' , and c^{j_0} lie in a same vertical plane of passing by $0z$, the ordering is completed by increasing colatitudes:

$$\begin{aligned} \min_j \{\langle c, c^j \rangle\} = \langle c, c^{j_0} \rangle = \min_p \{\langle c', c^p \rangle\} = \langle c', c^{j_0} \rangle \quad \text{and} \\ \text{either } \psi(c) < \psi(c') \\ \text{or } \psi(c) = \psi(c') \quad \text{and } \theta(c) < \theta(c'). \end{aligned} \quad (11)$$

The three relations (9) to (11) provide the unit sphere of \mathbb{R}^3 with a total ordering representing the chosen poles, and which is easy to compute. In the simpler case of a unique pole α it suffices to take it as north pole, and to take the sum $\theta + \psi$ for Voronoi distance (see below).

5 4-D Segmentations of “Pavie” Image

The image under study, kindly provided by J. Chanussot, represents the university of Pavia. It is composed of 103 bands from 0.43 to 0.86 micrometers. It has already been studied and classified [6]. The first principal component is depicted in Fig.3a, and the three next ones in Fig.2. Their variances are 64.84%, 28.41%, 5.14%, and 0.51% respectively.

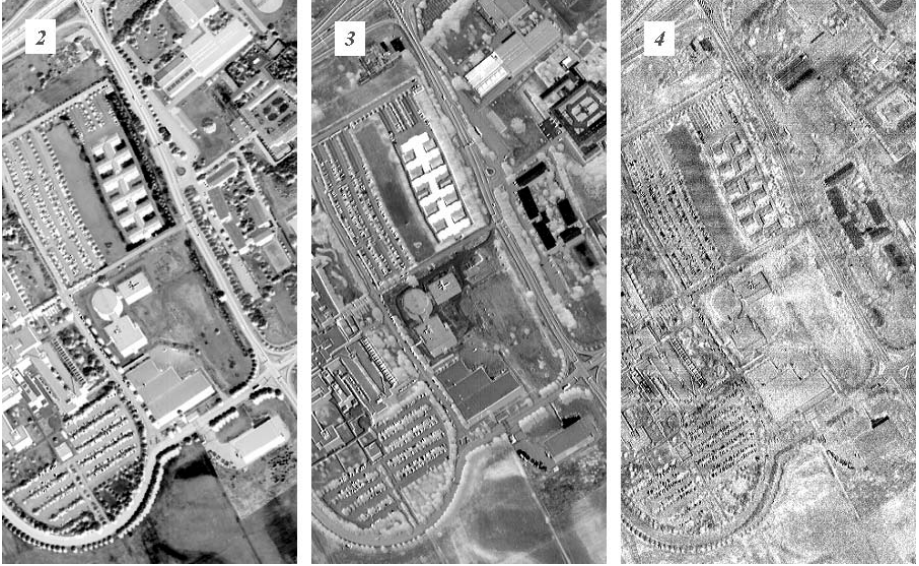


Fig. 2. Principal components n° 2, 3, and 4 of “Pavia” image

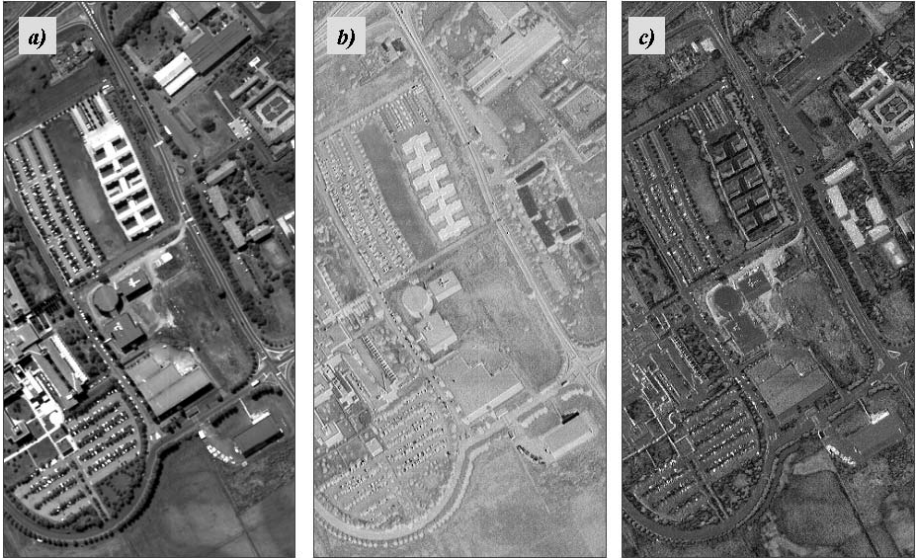


Fig. 3. a) First principal component of “Pavia” image; b) saturation \mathbb{R}^4 ; c) sum of the hues on the unit sphere of \mathbb{R}^3

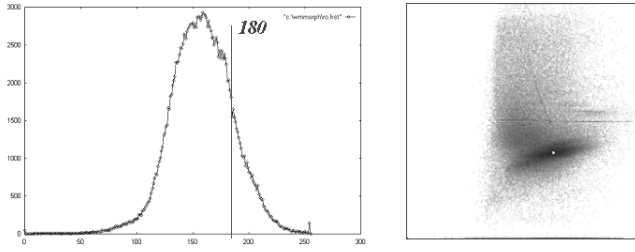


Fig. 4. Histogram of “Pavia” saturation ρ in \mathbb{R}^4 (left), and bidimensional histogram of the two hues θ and ψ (right)

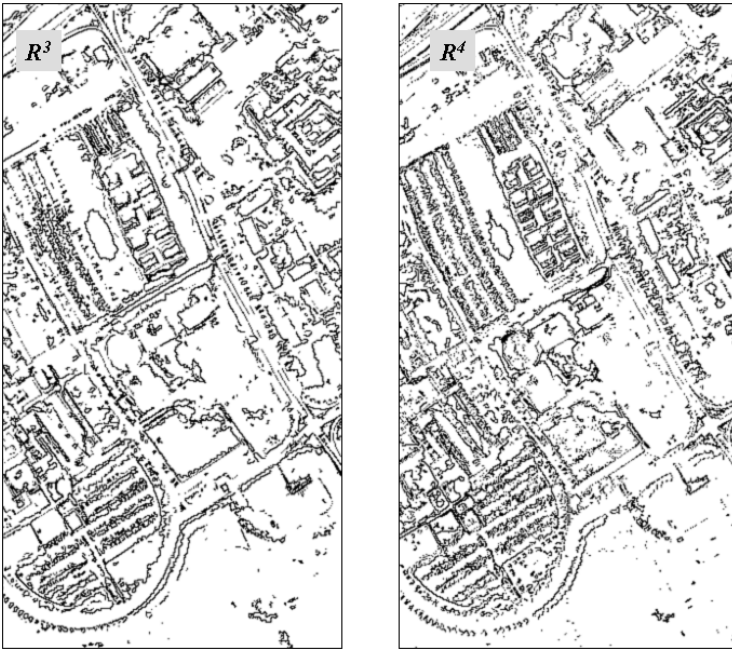


Fig. 5. Composite segmentations from the three (\mathbb{R}^3) or four (\mathbb{R}^4) first principal components of “Pavia”

The first component is the axis for polar cylindrical coordinates in \mathbb{R}^4 . In the perpendicular \mathbb{R}^3 space, saturation is given by the vector module ρ of Rel.6, and depicted in Fig.3b. Fig.4, left, depicts its histogram. It is unimodal, and its threshold at 180, for separating the zones of more representative hue, versus luminance, was set from the images themselves. The 2-D histogram of the two hues θ and ψ (Fig.4, right) is sufficiently unimodal for extracting the single pole of $\theta = 159$ and $\psi = 162$, indicated in white on the histogram. By taking for distance on the unit sphere the sum of the distances according θ and ψ , with θ

prioritary, we establish a total ordering \mathcal{O}_{hue} on the unit sphere. It results in a unique hue, represented in Fig.3c. The whole 4-D lattice is given by the product $\mathcal{T}_{lum} \otimes \mathcal{T}_{sat} \otimes \mathcal{T}_{hue}$ where \mathcal{T}_{hue} is the lattice associated with \mathcal{O}_{hue} .

The composite segmentation is performed according to the technique already presented in [1]. The luminance of Fig. 3a is segmented by iterated jumps (jump=25) and merging of small particles fusion (area ≤ 5), Similarly the hue of Fig. 3c is segmented by jumps of 35, and merging 5. Saturation ρ of Fig. 3b is used as a local criterion for choosing between the partitions of the luminance and of the hue. The final composite partition is depicted in Fig.5. By comparing with the same technique applied to the first three components only, we observe that the fourth dimension allowed us to segment several supplementary details, in particular in the bottom of the image.

6 Conclusion

A technique for piloting some variables by another ones in multivariable lattices has been proposed. It led us to establish total orderings on the unit sphere that are significative in remote sensing. One can probably free oneself from the discrete assumption, by modelling all numerical variable by Lipschitz functions. Applications of the method to GIS problems are foreseen.

Acknowledgements. The author wish to thank Ch. Ronse, J. Angulo and S. Lefèvre for their valuable comments, and J. Chanussot and Y. Tarabalka for the use of “Pavia” image.

References

1. Angulo, J., Serra, J.: Modeling and segmentation of colour images in polar representations. *Image and Vision Computing* 25, 475–495 (2007)
2. Angulo, J.: Quaternions colour representation and derived total orderings for morphological operators. *Note interne CMM* (May 2008)
3. Aptoula, E., Lefèvre, S.: A comparative study on multivariate morphology. *Pattern Recognition* 40(11), 2914–2929 (2007)
4. Aptoula, E.: Analyse d’images couleur par morphologie mathématique, application à la description, l’annotation et la recherche d’images Thèse d’informatique. Univ. Louis Pasteur, Strasbourg (July 10, 2008)
5. Chanussot, J., Lambert, P.: Total ordering based on space filling curves for multi-valued morphology. In: *ISMM 1998*, Norwell, MA, USA, pp. 51–58. Kluwer Academic Publishers, Dordrecht (1998)
6. Chanussot, J., Benediktsson, J.A., Fauvel, M.: Classification of Remote Sensing Images from Urban Areas Using a Fuzzy Possibilistic Model. *IEEE Trans. Geosci. Remote Sens.* 3(1), 40–44 (2006)
7. Ell, T.A., Sangwine, S.J.: Hypercomplex Fourier transform of color images. *IEEE Trans. Image Processing* 16(1), 22–35 (2007)
8. Evans, A., Gimenez, D.: Extending Connected Operators To Colour Images. In: *Proc. Int. Conf. Image Proc.* 2008, pp. 2184–2187 (2008)

9. Hanbury, A., Serra, J.: Morphological operators on the unit circle. *IEEE Trans. Image Processing* 10(12), 1842–1850 (2001)
10. Hanbury, A., Serra, J.: Colour Image Analysis in 3D-polar coordinates. In: Michaelis, B., Krell, G. (eds.) *DAGM 2003. LNCS*, vol. 2781, pp. 124–131. Springer, Heidelberg (2003)
11. Meyer, F.: Color image segmentation. In: *Proc. 4th International Conference on Image Processing and its Applications 1992*, pp. 303–306 (1992)
12. Serra, J.: Les treillis pilotes. *Rapport Technique CMM-Ecole des Mines de Paris* (January 2009)
13. Soille, P.: Constrained connectivity for hierarchical image partitioning and simplification. *IEEE Trans. PAMI* 30(7), 1132–1145 (2008)
14. Talbot, H., Evans, C., Jones, R.: Complete ordering and multivariate mathematical morphology: Algorithms and applications. In: *ISMM 1998, Norwell, MA, USA*, pp. 27–34. Kluwer Academic Publishers, Dordrecht (1998)